HHS Public Access

Author manuscript

J Physiol. Author manuscript; available in PMC 2024 February 16.

Published in final edited form as:

J Physiol. 2023 December ; 601(23): 5277–5293. doi:10.1113/JP285259.

Modulation of sarcopenia phenotypes by glutathione peroxidase 4 overexpression in mice

Hongyang Xu[1], **Agnieszka Czyżowska**[1], **Holly Van Remmen**[1,2], **Jacob L. Brown**[1,2]

[1]Aging and Metabolism Research Program, Oklahoma Medical Research Foundation, Oklahoma City, OK, USA

[2]Oklahoma City VA Medical Center, Oklahoma City, OK, USA

Abstract

Our laboratory previously showed lipid hydroperoxides and oxylipin levels are elevated in response to loss of skeletal muscle innervation and are associated with muscle pathologies. To elucidate the pathological impact of lipid hydroperoxides, we overexpressed glutathione peroxidase 4 (GPx4), an enzyme that targets reduction of lipid hydroperoxides in membranes, in adult CuZn superoxide dismutase knockout (*Sod1*KO) mice that show accelerated muscle atrophy associated with loss of innervation. The gastrocnemius muscle from *Sod1*KO mice shows reduced mitochondrial respiration and elevated oxidative stress (F_2-isoprostanes and hydroperoxides) compared to wild-type (WT) mice. Overexpression of GPx4 improved mitochondrial respiration and reduced hydroperoxide generation in *Sod1*KO mice, but did not attenuate the muscle loss that occurs in *Sod1*KO mice. In contrast, contractile force generation is reduced in EDL muscle in *Sod1*KO mice relative to WT mice, and overexpression of GPx4 restored force generation to WT levels in *Sod1*KO mice. GPx4 overexpression also prevented loss of muscle contractility at the single fibre level in fast-twitch fibres from *Sod1*KO mice. Muscle fibres from *Sod1*KO mice were less sensitive to both depolarization and calcium at the single fibre level and exhibited a reduced activation by *S*-glutathionylation. GPx4 overexpression in *Sod1*KO mice rescued the deficits in both membrane excitability and calcium sensitivity of fast-twitch muscle fibres. Overexpression of GPx4 also restored the sarco/endoplasmic reticulum Ca^{2+}-ATPase activity in *Sod1*KO gastrocnemius muscles. These data suggest that GPx4 plays an important role in

Corresponding authors H. Van Remmen: Aging and Metabolism Research Program, Oklahoma Medical Research Foundation, 825 N.E. 13th Street, Oklahoma City, OK 73104, USA. holly-vanremmen@omrf.org, J. L. Brown: Oklahoma City VA Medical Centre, 921 N.E. 13th Street, Oklahoma City, OK 73104, USA. jacob-brown@omrf.org.

Author contributions

All experiments were performed in H.V.R. and J.L.B.'s laboratory. Conception or design of the work: H.X., H.V.R., and J.L.B. Acquisition, analysis or interpretation of data for the work: H.X., A.C. and J.L.B. All authors have read and approved the final version of this manuscript and agree to be accountable for all aspects of the work in ensuring that questions related to the accuracy or integrity of any part of the work are appropriately investigated and resolved. All persons designated as authors qualify for authorship, and all those who qualify for authorship are listed.

The peer review history is available in the Supporting Information section of this article (https://doi.org/10.1113/JP285259#support-information-section).

Additional information

Competing interests

All authors declare no conflicts of interest.

Supporting information

Additional supporting information can be found online in the Supporting Information section at the end of the HTML view of the article. Supporting information files available:

preserving excitation–contraction coupling function and Ca^{2+} homeostasis, and in maintaining muscle and mitochondrial function in oxidative stress-induced sarcopenia.

Graphical Abstract

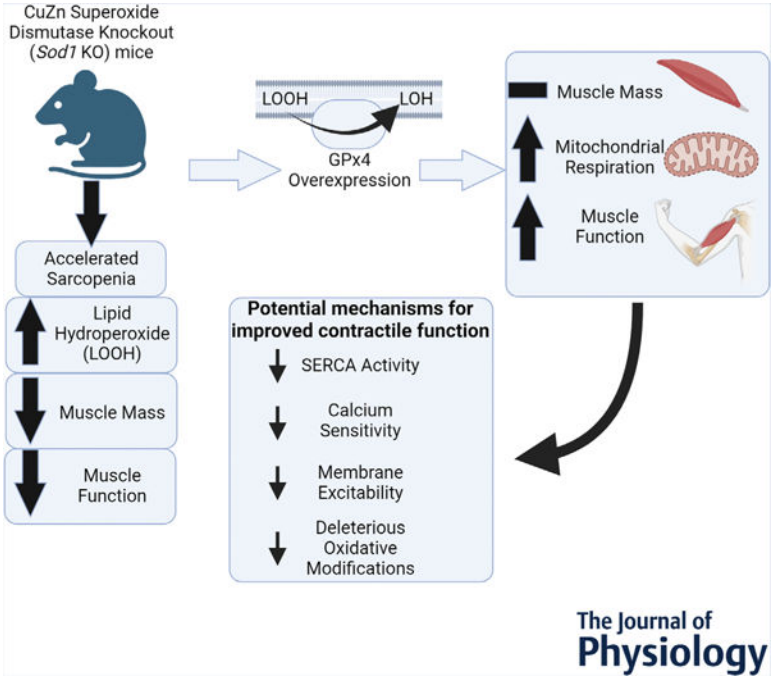

Summary of the findings of the work. GPx4, glutathione peroxidase 4; SERCA, sarco/endoplasmic reticulum Ca^{2+} ATPase; Sod1, CuZn superoxide dismutase.

Keywords

Ca^{2+} sensitivity; E–C coupling; lipid peroxidation; mitochondria; muscle function; oxidative stress; SERCA activity

Introduction

Sarcopenia is characterized by progressive loss of skeletal muscle mass and strength with an increased risk of adverse outcomes such as physical disability, poor quality of life and even death (Goodpaster et al., 2006). Oxidative stress is a key contributing factor to sarcopenia. Briefly, researchers have previously linked oxidative stress to impaired contractile function, muscle degradation and mitochondrial dysfunction (Andrade et al., 1998; Plant et al., 2001). The Cu/Zn superoxide dismutase knockout (*Sod1*KO) mouse is a model of sarcopenia that exhibits high levels of oxidative stress and damage due to loss of superoxide scavenging capacity. We have characterized this model extensively, reporting muscle atrophy and weakness that resembles the ageing muscle phenotypes present in old wild-type mice in an accelerated time frame. Specifically, *Sod1*KO mice show a significant loss of muscle innervation, lower muscle mass and reduced muscle contractile function (Deepa et al., 2017). We have also shown that *Sod1*KO mice have reduced fibre Ca^{2+} sensitivity associated

with irreversible oxidative modifications on troponin I (TnI) on contractile filaments, decreased sarco/endoplasmic reticulum Ca^{2+}-ATPase (SERCA) activity, increased cytosolic Ca^{2+} concentration, compromised sarcoplasmic reticulum (SR) Ca^{2+} storage, impaired ryanodine receptor (RyR, SR Ca^{2+} release channel) structure and blunted membrane excitability with altered levels of Na^{+},K^{+}-ATPase (NKA, membrane potential keeper) (Xu et al., 2022). These adverse oxidative modifications related to excitation–contraction (E–C) coupling and Ca^{2+} regulating systems in skeletal muscle contribute to muscle weakness (Qaisar et al., 2018) and mirror changes seen in ageing skeletal muscle.

Our laboratory has also demonstrated that lipid hydroperoxides are elevated in skeletal muscle from aged mice and *Sod1*KO mice (Loehr et al., 2016; Muller et al., 2007), and the production of lipid hydroperoxides is correlated to the extent of muscle loss (Brown et al., 2022; Pharaoh et al., 2020). We have also shown that overexpression of glutathione peroxidase 4 (GPx4) ameliorates sarcopenia (Czyżowska et al., 2023). Lipid peroxidation can damage cellular components, in particular membranes, and can lead to the production of toxic signalling molecules such as 4-hydroxynonenal (4-HNE) (Schwarzer et al., 2015), which has been shown to trigger skeletal muscle pathology (Schwarzer et al., 2015). To define the role of lipid hydroperoxides in muscle atrophy and weakness, we asked whether overexpression of the phospholipid hydroperoxidase GPx4, an antioxidant enzyme that has the unique ability to neutralize lipid hydroperoxides in membranes, can alter the oxidative stress-induced sarcopenia phenotypes present in the *Sod1*KO mice (Brigelius-Flohé, 1999). Our laboratory has shown that overexpression of mitochondrial hydroperoxide scavengers such as catalase does not protect against denervation-induced muscle loss (Pharaoh et al., 2020), while overexpression of GPx4 reduces denervation-induced muscle loss (Bhattacharya et al., 2009). However, it is not known if overexpression of GPx4 can mitigate sarcopenia phenotypes in *Sod1*KO mice.

We hypothesized that reducing lipid peroxide levels through overexpression of GPx4 would protect muscle mass, muscle force generation and mitochondrial respiration in denervation-induced sarcopenia. To test this hypothesis, we crossed whole body *Sod1*KO mice with GPx4 transgenic mice and measured muscle mass, muscle function, hydroperoxide generation and mitochondrial respiration. The results from this study can help us narrow our focus for future interventions for sarcopenia.

Methods

Ethical approval

All animal experiments were conducted in accordance with the guidelines for the care and use of laboratory animals of the Oklahoma Medical Research Foundation (OMRF). Institutional Animal Care and Use Committees (IACUC) at OMRF has approved this study (approval number 19–53). We conducted experiments using male and female mice from strains on a C57BL/6J genetic background currently housed in the mouse colony of Dr Van Remmen at the OMRF. Further, all authors confirm that the experiments described in this article conform to the principles and regulations described in the editorial by Grundy (Grundy, 2015).

Animals

To generate the mouse model, we crossed *Sod1*KO mice with GPx4 transgenic mice. We have described the breeding and characterization of the *Sod1*KO mice in detail elsewhere (Muller et al., 2006). The GPx4 transgenic mice were generated using a genomic clone containing the human GPx4 gene, as described in detail by Ran et al. (2004). We identified mice using PCR genotyping. We sacrificed mice using CO_2 asphyxiation at a fill rate between 30% and 70% of the chamber volume per minute followed by cervical dislocation. For all studies except the single fibre contractility studies, we euthanized mice at 17–18 months of age. At sacrifice we drew blood through the aorta, and collected tissues, which were snap frozen in liquid nitrogen for subsequent analyses. In previous studies we have shown that the *Sod1*KO mice at this age show sarcopenia phenotypes comparable to old (25–28 months) wild-type mice (Deepa et al., 2019; Jang et al., 2010; Larkin et al., 2011; Muller et al., 2006). For the single fibre contractility analysis, we sacrificed mice at 8 months of age as we had shown in a previous study that E–C coupling function is impaired in muscle fibres from *Sod1*KO mice at this age (Xu et al., 2022). The number of animals used was determined based on our previous studies using the *Sod1*KO mice (Ahn et al., 2022; Qaisar et al., 2019; Xu et al., 2021). We chose to use female mice for this study because male mice were used as breeders.

Ex vivo extensor digitorum longus contractility

Contractile properties were measured in the extensor digitorum longus (EDL) muscle as previously described (Qaisar et al., 2018). Briefly, the EDL muscle was suspended on a dual-mode muscle lever system (300C-LR, Aurora Scientific Inc, Aurora, ON, Canada) using a hook in Krebs buffer. The muscle was placed at optimal length and allowed 20 min for thermoequilibration at 32°C. A supramaximal current (600–800 mA) of 0.25 ms pulse duration was delivered through a stimulator (701 C, Aurora Scientific Inc.), and the train duration for isometric contractions was 300 ms. We recorded and analysed data using commercial software (DMC and DMA, Aurora Scientific). Specific force (N/cm^2) of EDL muscles was calculated using the ratio of fibre length to muscle length as published previously (Qaisar et al., 2018). EDL muscle was used for contractility assays while gastrocnemius muscle was used for other biochemical assays to avoid any effect from stimulation. Our previous studies show that the EDL muscle is susceptible to contractile dysfunction in the *Sod1*KO mouse model and in ageing wild-type mice (Qaisar et al., 2018).

Preparation of skinned fast-twitch single muscle fibres

The EDL muscle was excised and used as a source of single skinned fast-twitch muscle fibre segments. As described previously (Xu et al., 2018), after the dissection, the EDL muscle was pinned at resting length at room temperature under the paraffin oil on a Sylgard layer and kept cool on an ice pack (~10°C). We dissected single muscle fibre segments under a light microscope, and the sarcolemma was removed by mechanically skinning the fibre segment using fine forceps, as described previously (Xu et al., 2018). We mounted the skinned fibre segment between a forceps and transducer (TR5S, Myotronic, Heidelberg, Germany) provided with the skinned muscle-station (Myotronic) at the resting length (i.e. length just less than that eliciting measurable passive force). Sarcomere length was measured

by the laser diffractions provided with the station, and there is no difference observed across three different groups (all sarcomere lengths are around 2.5 μm). The fibre type of each skinned single fibre was determined by exposure to strontium solution at pSr 5.2 at the end of each experiment. Type II fibres produce very little force at pSr 5.2, whereas type I fibres produce >80% of the maximum force as previously described (Xu et al., 2018). Based on the muscle contractile parameters measured at whole muscle level, there is no difference in muscle mass or force production between wild-type (WT) and WT/GPx4Tg groups, and therefore measurements at single fibre level did not include the WT/GPx4Tg group.

All chemicals used for single fibre manipulations were from Sigma-Aldrich (St Louis, MO, USA) unless otherwise stated. We used heavily Ca^{2+}-buffered solutions for examining the contractile properties of single fibres. These included a 'relaxing solution', containing (in mM): 126 K^+, 36 Na^+, 1 Mg^{2+}, 90 HEPES, 50 EGTA, 8 ATP, 10 creatine phosphate, pH 7.10, pCa > 9, osmolality of 295±10 mosmol/kg H_2O, and a 'maximal Ca^{2+}-activating solution' that is very similar but with 50 mM CaEGTA (at pCa ~4.7) instead of EGTA (Xu et al., 2018). For assessing fibre type as mentioned above, we made a strontium-based solution at pSr 5.2 which is similar to 'maximal Ca^{2+}-activating solution', but with Sr^{2+} instead of Ca^{2+}. We mixed this solution with 'relaxing solution' at a ratio of 1:7. K-HDTA (hexa-methylene-diamine-tetraacetate) solution (like relaxing solution but with HDTA replacing EGTA) was used to examine E–C coupling (membrane excitability). Additionally, we used a Na-HDTA solution, similar to the K-HDTA solution by replacing K^+ with Na^+ (achieved by adjusting pH with NaOH instead of KOH), to depolarize the transverse tubules in skinned muscle fibres.

Single skinned fibre measures

Measurement of contractile apparatus parameters (maximum specific force and calcium sensitivity).—After the skinned fibre segment was mounted onto the transducer and sarcomere length measured as described above, we stretched the fibre to 120% of its resting length and transferred it into a Perspex bath containing 2 ml of relaxing solution for 2 min. The fibre was activated in a sequence of solutions with progressively higher levels of free [Ca^{2+}] (pCa ~9 to 4.7), with maximum force produced at pCa 4.7. We recorded force with a bridge amplifier (Myotronic) and the Aurora Data Acquisition Signal Interface (604A) with DMC software. The maximum specific force (in mN/mm^2) was then calculated by normalizing the maximum Ca^{2+}-activated force (mN) of the fibre to its cross-sectional area (mm^2), and the fibre cross-sectional area (in mm^2) was calculated by measuring the fibre diameter in three different places along the length of the fibre (Xu et al., 2018). After going through the sequence, we moved the fibre back into relaxing solution where it fully relaxed again. We repeated such force–pCa staircases two to three times for each fibre. We expressed the force at each [Ca^{2+}] within a given sequence as a percentage of the corresponding maximum force, and the data were fitted with a Hill curve (force–pCa curve), using GraphPad Prism 9 software (GraphPad Software, Boston, MA, USA). Based on this force–pCa curve, the pCa_{50} value was calculated in order to compare the Ca^{2+} sensitivity of contractile apparatus from different fibres. pCa_{50} is the calcium concentration at which the given fibre produces half of its maximum force. This can be used to compare

fibre Ca^{2+} sensitivity, independent of variations in maximum force in fibres with different sizes.

To induce *S*-glutathionylation on troponin I (TnI), fibres were treated with 2,2′-dithiodipyridine (DTDP)–reduced glutathione (GSH). We diluted a 100 mM stock solution of GSH in K-HDTA solution 20-fold to a final concentration of 5 mM. A solution of DTDP in absolute ethanol at 100 mM was diluted 1000-fold to a final concentration of 100 μM. This small amount of ethanol (0.1%) had no effect compared to controls without ethanol. Briefly, after measuring force–pCa staircases, we treated fibres with 100 μM DTDP for 5 min, and then treated with 5 mM GSH for 2 min. We then treated the fibre with the force–pCa test again, and the pCa_{50} values were calculated based on the new staircases, to compare with the old values before the treatment.

Measurement of membrane excitability.—Membrane excitability was examined in skinned single fast-twitch fibres through the detection of depolarization-induced force responses. When we mechanically skinned a muscle fibre, the transverse (t) system seals off. The t-system can become polarized again when the fibre is placed in the standard K-HDTA solution, because the action of NKA in the t-system membrane establishes a high Na^+ concentration and a low K^+ concentration within the t-system (Lamb, 2002). If the t-system is sufficiently well polarized, the voltage sensors (dihydropyridine receptors, DHPR) in the t-system return to an activatable state, and if the skinned fibre is subsequently transferred into the zero potassium (Na-HDTA) solution, the t-system is rapidly depolarized, activating the voltage sensors, which in turn trigger Ca^{2+} release from the SR and a resultant force response (Lamb, 2002). Thus, we used the magnitude of the depolarization-induced response in a skinned fibre (relative to the maximum Ca^{2+}-activated force in that fibre) as a measure of the polarization of the t-system membrane and excitability of that fibre.

Muscle fibre permeabilization, oxygen consumption and hydroperoxide production rate measurement.—We prepared permeabilized red gastrocnemius muscle fibre bundles with saponin and measured oxygen consumption and hydroperoxide production with Amplex UltraRed using the Oroboros Oxygraph-2k (O2k, OROBOROS Instruments, Innsbruck, Austria) with a fluorometer as previously described (Brown et al., 2020). We measured hydroperoxide generation and respiration in the O2k.

SERCA pump activity.—SERCA activity was measured in muscle homogenates at 37°C using a spectrophotometric assay as previously described (Ahn et al., 2022). In brief, we homogenized all muscle samples following the ratio 1:10 with the SERCA homogenizing buffer, containing (in mM): 250 sucrose, 5 HEPES, 0.2 phenylmethylsulfonyl fluoride, 0.2% NaN_3. After centrifugation of the homogenates, we took the supernatant with the protein amount of 100 μg and mixed it with the SERCA assay buffer containing (in mM) 200 KCl, 20 HEPES, 10 NaN_3, 1 EGTA, 15 $MgCl_2$, 5 ATP and 10 phospho-enolpyruvate, to generate a 3 ml mixture; 18 U/ml of lactate dehydrogenase and pyruvate kinase was added along with 1 mM Ca^{2+} ionophore A-23187 (C-7522; Sigma) into the mixture. This reaction mixture was aliquoted and mixed with $CaCl_2$ to form eight different calcium concentrations with pCa points from 7.6 to 4.2 and a blank, and then loaded into a pre-warmed 37°C quartz plate. The reaction was initiated by adding 1 mM NADH into the mixture, and we performed

the kinetic assay by the following settings: temperature = 37°C, time = 30 min, $\lambda = 340$ nm (shaking between readings). We calculated the SERCA activity using the formula:

$$\text{Total ATPase rate} = \frac{\text{rate of } A_{340\text{nm}} \text{ signal loss}}{\text{pathlength} \times 6.23\text{mM}^{-1}\,\text{cm}^{-1}}$$

RNA isolation and quantitative real-time PCR

A quantitative real-time polymerase chain reaction (RT-PCR) was performed as previously described (Brown et al., 2020). We extracted total RNA from gastrocnemius using TRI reagent solution (Thermo Fisher Scientific, Waltham, MA, USA). We converted equal amounts of extracted RNA (1 μg) to first strand cDNA using a cDNA synthesis kit. We measured mRNA content for *Atrogin-1* and *MuRF-1* via RT-PCR by Quant Studio 6 Flex (Thermo Fisher Scientific). We used the $\Delta\Delta C_t$ method to calculate relative mRNA content.

Western blot analysis

We performed western blots as previously described (Brown et al., 2020). Briefly, gastrocnemius muscle was homogenized in radioimmunoprecipitation assay buffer. Protein concentrations were determined using a Bradford assay. We resolved 20–40 μg of protein by SDS-PAGE, transferred to a nitrocellulose membrane and blocked in 5% (w/v) bovine serum albumin in Tris-buffered saline with 0.2% Tween 20. We probed membranes overnight for antibodies specific to GPx4 (Santa Cruz Biotechnology, Dallas, TX, USA, cat. no. sc-166120, 1:1000), Sod1 (Enzo Life Sciences, Farmingdale, NY, USA, cat. no. ADI-SOD-101-E, 1:1000), and membrane excitability related proteins, RyR (Developmental Studies Hybridoma Bank (DSHB), Iowa City, IA, USA, cat. no. 34C, 1:1000), calstabin (Abcam, Waltham, MA, USA, cat. no. ab2918), DHPR (DSHB, cat. no. IIID5E1, 1:1000), NKAα1 (Cell Signaling Technology, Danvers, MA, USA, cat. no. 3010, 1:1000) and NKAα2 (Merck Millipore, Burlington, MA, USA, cat. no. 07–674, 1:1000). In the western blotting analysis for NKA, we probed for the NKAα1 isoform first, imaged the results and then stripped the membrane with stripping buffer (0.1 M glycine, 20 mM magnesium acetate, 50 mM KCl, pH 2.2) and re-probed with NKAα2. The total NKA amount was quantified by adding the quantified densitometric values of both NKAα1 and NKAα2 from the same membrane. We performed imaging with G: BOX imaging system (Syngene, Frederick, MD, USA) and quantified using Alpha View (Protein Simple BioTechne, Minneapolis, MN, USA) analysis software.

Statistical analysis

For animal experiments, independent factors were genotype (WT and *Sod1*KO) and genotype (WT and GPx4Tg). Therefore, experimental groups were WT/WT, *Sod1*KO/WT, WT/GPx4Tg and *Sod1*KO/GPx4Tg. A two-way ANOVA was employed as the global analysis for each dependent variable for animal experiments. For the individual fibre experiments, independent factors were genotype (WT, *Sod1*KO and *Sod1*KO GPx4Tg). We used a one-way ANOVA for the global analysis for each dependent variable in the skinned fibre experiments. For the single fibre experiments, we took several different fibres from three to four mice in each group. We pooled all the single fibres from all the animals and

counted each one as a datapoint for the single fibre studies. Where we found significant *F*-ratios, differences among means were determined by Tukey–Kramer *post hoc* test for both the animal and cell culture experiments. For all experiments, the comparison-wise error rate, α, was set at 0.05 for all statistical tests. We performed an outlier test at 99% confidence for all experiments, and we removed outliers. All data passed the normal distribution and equal variance assumptions of ANOVA. We analysed data and compiled figures using GraphPad Prism and data are expressed as means ± SD.

Results

Characterization of the *Sod1*KO/GPx4Tg experimental model

Figure 1A confirms the deletion of CuZnSOD protein in gastrocnemius of the *Sod1*KO and *Sod1*KO/Gpx4Tg models. Figure 1B shows human GPx4 mRNA was present in GPx4Tg mice, but not WT/WT and *Sod1*KO/WT mice. There was a main effect of GPx4 overexpression showing that GPx4 protein content is greater in GPx4Tg mice ($P = 0.0019$, Fig. 1C and D). Genotype was confirmed for all the mice used throughout the article. n = 5–11 per group was used for experiments in Fig. 1.

Overexpression of GPx4 does not protect against muscle atrophy in *Sod1*KO mice

We hypothesized that lipid hydroperoxides generated in response to denervation contribute to muscle atrophy, and thus overexpression of Gpx4 would reduce muscle atrophy in the *Sod1*KO mouse mice. We measured bodyweight and muscle wet weights in the four groups of mice at 17–18 months of age. There was a main effect of *Sod1*KO showing that bodyweights of *Sod1*KO mice were significantly smaller than WT/WT or WT/GPx4Tg mice ($P < 0.0001$, Fig. 2A). There was a main effect of *Sod1* deletion showing that the mass of the gastrocnemius and tibialis anterior muscle (TA) muscle was smaller measured as absolute wet weight and normalized to bodyweight when compared to WT/WT and WT/GPx4Tg mice ($P < 0.0001$ Fig. 2B–E). Further there was also a main effect showing that GPx4Tg increased muscle mass relative to WT/WT and *Sod1*KO/WT in TA muscle normalized to bodyweight ($P = 0.0397$, Fig. 2E). In soleus muscle, there was a main effect indicating that raw soleus weight was lower in *Sod1*KO mice when compared to WT/WT and WT/GPx4Tg mice ($P < 0.0001$, Fig. 2F). When normalized to bodyweight soleus wet weights were not different between groups (Fig. 2G). There was also a main effect showing both *Sod1* deletion and GPx4 overexpression reduced raw extensor digitorum longus (EDL) absolute wet weights ($P = 0.0015$ and $P = 0.0327$, respectively Fig. 2H). In the EDL, there wasa main effect indicating that weights normalized to bodyweight were lower in GPx4 Tg mice when compared to WT/WT and *Sod1*KO/WT mice ($P = 0.0347$, Fig. 2I). Finally, there was a main effect showing absolute wet weights of quadriceps muscle were significantly lower in *Sod1*KO mice when compared to WT/WT and WT/GPx4 Tg mice ($P = 0.0029$), but quadriceps wet weights were not different when normalized to bodyweight (Fig. 2J and K). n = 5–11 per group was used for experiments in Fig. 2.

Overexpression of GPx4 in *Sod1*KO mice improves mitochondrial respiration, reduces oxidative damage, and reactive oxygen species generation

Mitochondrial dysfunction is an underlying contributor to a variety of muscle pathologies (Abrigo et al., 2019); therefore, we wanted to determine if overexpression of GPx4 could reduce mitochondrial pathologies present in *Sod1*KO mice. We measured mitochondrial respiration and hydroperoxide production using permeabilized muscle fibres as we have previously described (Brown et al., 2020). The data showed an interaction indicating that maximally stimulated respiration (complex I + II) was reduced ~25% in fibres from *Sod1*KO mice compared to WT counterparts, while respiration was not reduced in muscle from *Sod1*KO mice with GPx4 overexpression ($P = 0.0142$, Fig. 3A). As a marker for oxidative stress in muscle, we measured F_2-isoprostanes. We report a main effect showing F_2-isoprostane levels were higher in muscle from *Sod1*KO mice compared to WT/WT and WT/GPx4Tg mice ($P = 0.0002$, Fig. 3B). There were main effects showing gastrocnemius mitochondrial production of hydroperoxides in the basal state (no substrates or ADP) was greater in fibres from *Sod1*KO mice when compared to WT counterparts ($P = 0.003$), and that GPx4 overexpression reduced hydroperoxides relative to WT/WT and *Sod1*KO/WT mice ($P = 0.0274$, Fig. 3C). $n = 4–8$ per group was used for experiments in Fig. 3.

Overexpression of GPx4 improves contractile function in EDL muscle in *Sod1*KO mice

Prior studies have shown that *Sod1*KO mice have reduced muscle force generation (Qaisar et al., 2018, 2019). Therefore, we wanted to determine if overexpression of GPx4 can modify contractile dysfunction in *Sod1*KO mice. There was an interaction showing maximum force was ~30% lower in *Sod1*KO mice when compared to WT mice, and that GPx4 overexpression increased maximum force by ~20% in *Sod1*KO mice ($P = 0.0401$, Fig. 4A). There was a main effect of *Sod1* deletion showing specific force was reduced when compared to WT/WT and WT/GPx4Tg mice ($P < 0.0001$, Fig. 4B). There was also a main effect showing that specific force was greater in GPx4Tg mice relative to WT/WT and *Sod1*KO/WT mice ($P = 0.0103$, Fig. 4B). $n = 5–8$ animals per group was used for Fig. 4A and B.

To explore the mechanisms by which overexpression of GPx4 improves contractile function at the single muscle fibre level in *Sod1*KO mice, we utilized a skinned single muscle fibre model that allows us to specifically measure the activation and calcium sensitivity of muscle contractile function at the level of contractile proteins. The main effect of *Sod1* deletion showed a decreased specific force by ~25% in *Sod1*KO skinned muscle fibres compared to skinned fibres from WT mice ($P < 0.0001$). There was also an effect showing the overexpression of GPx4 in *Sod1*KO fibres blunted the decrease in specific force observed in *Sod1*KO mice ($P = 0.0032$, Fig. 4C, $n = 11–14$ fibres analysed, $n = 3–4$ animals).

Overexpression of GPx4 improves calcium sensitivity of contractile filaments in fast-twitch fibres in *Sod1*KO mice, as well as the activating reaction to *S*-glutathionylation

We measured the calcium sensitivity of contractile filaments in single skinned fast-twitch muscle fibres by activating the contractile apparatus using a series of solutions with free [Ca^{2+}] heavily buffered at successively higher levels (pCa > 10 to pCa 4.7, denoted by arrows in Fig. 5A), to elicit progressively greater force production (Fig. 5A). Based on

these results, we plotted a force–pCa curve, showing a progressively greater force under the increasing Ca^{2+} concentration (Fig. 5B). Using the force–pCa curve, we obtained the pCa_{50}, which is the calcium concentration at which the fibre produces half of its maximum force. We used the pCa_{50} value to describe the calcium sensitivity of the muscle contractile apparatus. Our quantified data showed that in *Sod1*KO fibres, the pCa_{50} value (5.79) was significantly lower than in wild-type fibres (5.85) ($P = 0.0035$), indicating a decreased calcium sensitivity (Fig. 5C); and overexpression of GPx4 attenuated this blunted calcium sensitivity by increasing the pCa 50 value (5.84) ($P = 0.0116$) to a similar level compared to wild-type fibres. It has been previously shown that treatment with the sulfhydryl-specific oxidant 2,2′-dithiodipyridine (DTDP, 100 μM, 5 min) in combination with reduced glutathione (GSH, 5 mM, 2 min) (referred to as DTDP–GSH treatment) in skinned fast-twitch fibres results in *S*-glutathionylation of the troponin I (TnI) fast isoform (on the Cys134 residue) (Mollica et al., 2012). *S*-Glutathionylation can induce a significant increase in myofibrillar Ca^{2+} sensitivity, which is reversible by treatment with dithiothreitol (10 mM for 5 min) (Lamb & Posterino, 2003; Lamboley et al., 2015; Mollica et al., 2012). Our group has recently reported a significantly reduced reaction to this *S*-glutathionylation in *Sod1*KO fibres compared to wild-type fibres (Xu et al., 2022). To determine whether this impaired modification of TnI in *Sod1*KO fast-twitch fibres was attenuated by GPx4 overexpression, DTDP–GSH treatment was applied to skinned fast-twitch fibres from wild-type, *Sod1*KO and *Sod1*KO/GPx4Tg mice. We found an increased calcium sensitivity in *Sod1*KO fibres (0.11 pCa unit) that was significantly lower than the increase in wild-type fibres (0.14 pCa unit) ($P = 0.04$) in response to glutathionylation, suggesting inefficient modification of the Cys134 residue of TnI. The overexpression of GPx4 brought this blunted response to glutathionylation in *Sod1*KO fibres back to a similar level to wild-type fibres, with the pCa unit increased for 0.13 unit after the DTDP–GSH treatment (Fig. 5D, $P = 0.24$, $n = 8$–9 fibres analysed, $n = 3$–4 animals from which the fibres were obtained).

Membrane excitability is significantly impaired in fast-twitch fibres from *Sod1*KO mice and greatly improved by the overexpression of GPx4

We measured membrane excitability in single skinned fast-twitch muscle fibres from all three groups. In each skinned fibre, the membrane excitability was determined by recording the force response produced by the t-system depolarization through ionic substitution (upon exchange of K^+-HDTA with Na^+-HDTA) as described Methods. In normal conditions, t-system depolarization in fast-twitch fibres is able to trigger a force response as high as close to 80% of the maximum Ca^{2+}-activated force production in that fibre (Xu et al., 2018), which is what we found in the adult wild-type fibres (85%) (Fig. 6A and B). In contrast, the depolarization-induced force response was significantly lower in the *Sod1*KO fibres compared to adult wild-type fibres ($P < 0.0001$), triggering 29% of the maximum force (Fig. 6A and B). The main effect of overexpression of GPx4 improved the depolarization-induced force response in *Sod1*KO fibres, triggering 64% of the maximum force (Fig. 6A and B) ($P < 0.0001$, $n = 9$–22 fibres analysed, $n = 6$–7 animals from which the fibres were obtained).

GPx4 overexpression alters the expression of excitation related proteins in *Sod1*KO mice

To investigate possible mechanisms responsible for this alleviation by GPx4 overexpression, we measured the expression of proteins potentially involved in regulating membrane

excitability in whole gastrocnemius muscle homogenates, including the calcium release channel ryanodine receptor (RyR) and its stabilizer calstabin, voltage sensor dihydropyridine receptor α-subunit (DHPRα), and the membrane potential keeper Na^+,K^+-ATPase (NKA) through western blotting. RyR content was not changed across the three groups, but the RyR stabilizer calstabin was significantly lower in *Sod1*KO muscles compared to wild-type muscles ($P = 0.0048$), and overexpression of GPx4 eliminated this reduction (Fig. 7A and B) ($P = 0.0012$). DHPRα protein levels were significantly lower in *Sod1*KO ($P < 0.0001$) and *Sod1*KO/GPx4Tg ($P = 0.0335$) muscles compared to wild-type muscles, with the amount slightly better preserved in the muscles from *Sod1*KO/GPx4Tg mice compared to *Sod1*KO mice (Fig. 7C) ($P = 0.0001$). As the predominant catalytic subunit of NKA, the NKAα subunit has two major isoforms. NKAα1 is the ubiquitous isoform appearing in all tissues, and NKAα2 is the skeletal muscle specific isoform. Changes in the amount of NKAα indicate different levels of membrane potential, or an altered ability for maintaining or restoring membrane potential. We measured a significant reduction of the muscle specific NKAα2 amount in both *Sod1*KO (54% reduced, $P = 0.0064$) and *Sod1*KO/GPx4Tg ($P = 0.0415$) fibres (38% reduced) compared to wild-type muscle (Fig. 7E), while there was no change in the amount of the ubiquitous NKAα1 isoform across the three groups (Fig. 7D). However, the total amount of NKAα subunit showed a significant reduction in muscles from *Sod1*KO (37% reduced, $P = 0.0017$) and *Sod1*KO/GPx4Tg (23% reduced, $P = 0.0294$) mice (Fig. 7F, $n = 6–7$ animals). Representative images are shown to the right of the graphs.

Overexpression of GPx4 in *Sod1*KO mice improves SERCA activity

The activity of SERCA is responsible for rapidly returning calcium ions to the SR lumen and maintaining cellular calcium homeostasis. To explore the mechanism by which muscle calcium dysregulation in *Sod1*KO mice was restored in *Sod1*KO/GPx4Tg mice, we measured SERCA activity in gastrocnemius muscle homogenates. There was a significant decrease in SERCA activity in *Sod1*KO mice (30% reduction, $P = 0.0295$) when compared to WT mice, which was restored in the muscle of *Sod1*KO/GPx4Tg mice ($P = 0.05$) (Fig. 8A–B, $n = 6–7$ animals).

Discussion

Denervation of hindlimb muscle induces generation of lipid hydroperoxides and oxylipins that contribute to muscle atrophy (Bhattacharya et al., 2009; Brown et al., 2022; Pharaoh et al., 2020) but the mechanisms of muscle degeneration are unknown. Because the antioxidant enzyme GPx4 plays a critical role in reducing lipid hydroperoxides, particularly in membranes, we asked whether GPx4 overexpression could reduce or prevent muscle degeneration and weakness initiated by loss of innervation using the *Sod1*KO mouse model of sarcopenia. The *Sod1*KO mice have elevated oxidative stress and accelerated sarcopenia phenotypes including loss of muscle mass and function, neuromuscular junction (NMJ) degeneration, and elevated mitochondrial peroxide generation (Deepa et al., 2017). Here we show that overexpression of GPx4 can improve mitochondrial respiration and skeletal muscle function at both whole muscle and single muscle fibre levels in the *Sod1*KO mice. Specifically, overexpression of GPx4 reduces calcium dysregulation and improves the membrane excitability and restores the impaired E–C coupling system in

*Sod1*KO mice. Further, we showed that overexpression of GPx4 improved SERCA activity in gastrocnemius muscle from *Sod1*KO mice. However, overexpression of GPx4 did not preserve muscle mass in *Sod1*KO mice. These findings directly suggest that lipid hydroperoxides are a key contributor to mitochondrial and muscle contractile dysfunction under high oxidative stress in *Sod1*KO mice.

In the *Sod1*KO mice, the loss of muscle mass relative to wild-type mice is evident as early as 4–6 months of age (Deepa et al., 2017), and reaches more than 40% gastrocnemius muscle mass loss by 20 months of age compared to wild-type mice (Deepa et al., 2017). Consistent with ageing wild-type mice, the soleus muscle does not lose muscle mass in the *Sod1*KO mouse model (Jang et al., 2010; Muller et al., 2006). This is likely related to differences in fibre type composition between the soleus and other hindlimb muscles. The soleus contains more type I fibres that can contribute to a more robust antioxidant defence system than found in type IIA, B or X fibres in mouse muscle (Powers et al., 1994). In addition to the fibre type difference, the type I fibres in soleus muscle are innervated by slow fatigue-resistant motor neurons (SFR MN), which have been reported to be more resistant to oxidative stress compared to fast fatigable motor neurons (FF MN), and this resistance of SFR MN will slow the neurodegenerative impact to muscle atrophy due to oxidative stress or ageing (Kanning et al., 2010; Stifani, 2014). Interventions that preserve the NMJ and maintain innervation are effective protectors of muscle mass in *Sod1*KO mice (Ahn et al., 2022; Pharaoh et al., 2020; Xu et al., 2021). In fact, we recently showed that mitochondrial targeted expression of catalase in muscle from *Sod1*KO mice preserved the NMJ and inhibited denervation leading to maintenance of muscle mass and function (Xu et al., 2021). In contrast, the overexpression of the mitochondrial peroxide scavenger peroxiredoxin 3 (Prdx3) was ineffective in protecting the NMJ and only partially protected muscle mass, presumably from direct effects of mitochondrial peroxide production on muscle fibre (Ahn et al., 2022). Importantly, the specific force was protected in Prdx3×*Sod1*KO mice, supporting the protective effect of reducing peroxides on intrinsic aspects related to muscle force generation (Ahn et al., 2022). While these models invoked overexpression of hydrogen peroxide scavengers in the mitochondria (mitochondrial catalase (mCAT) and Prdx3), the current study in the GPx4 transgenic mice investigates the impact of protection from mitochondrial and cytosolic peroxides, and more specifically from lipid hydroperoxides that cause damage to membranes. In our previous studies we showed that the generation of lipid hydroperoxides occurs in response to loss of innervation, and is highly correlated to muscle atrophy (Brown et al., 2022; Pharaoh et al., 2020). To our surprise, overexpression of GPx4 did not protect against muscle loss in *Sod1*KO mice like the H_2O_2 scavengers mCAT and Prdx3. In the *Sod1*KO model, we see that the *Sod1*KO appears to cause a compensatory increase in many antioxidant proteins (Brown et al., 2020). Perhaps one reason why we did not see mass protection in the *Sod1*KO/GPx4Tg mice is because the high expression of human Gpx4 in the transgenic model has reached a compensatory threshold level that is not further increased by the lack of the *Sod1* gene in *Sod1*KO mice. Further, it is possible that the elevated expression of GPx4 may not have been able to offset the motor neuron component of the initiation of muscle atrophy in *Sod1*KO mice (i.e. loss of NMJ integrity and increased denervation of the muscle). However, in our recent paper we did observe a protection in muscle mass with GPx4 overexpression in aged mice (Czyżowska et al., 2023).

Scavenging lipid hydroperoxides does not change muscle mass in *Sod1*KO mice, but rather improves the muscle intrinsic processes in *Sod1*KO. There was protection from deleterious downstream pathways activated by loss of innervation, as evidenced by a protection in mitochondrial respiration, calcium handling and contractile mechanisms. Several studies have reported that GPx4 is important for mitochondrial function (Liang et al., 2007, 2009; Tadokoro et al., 2020). Here we showed that overexpression of GPx4 protected maximally stimulated mitochondrial respiration in gastrocnemius muscle from *Sod1*KO mice. This is also consistent with our prior studies showing that ATP production was preserved in GPx4 Tg mice following diquat treatment in livers (Liang et al., 2007). Further, overexpression of GPx4 prevents loss of mitochondrial membrane potential and ANT inactivation (IMAI et al., 2003; Yagi et al., 1998). Mitochondrial dysfunction isa hallmark of sarcopenia, so GPx4 may be critical to preserving muscle health during ageing (Ferri et al., 2020). Perhaps the most striking effect of GPx4 overexpression in the *Sod1*KO mice is the preservation of muscle contractile function at both the whole muscle and single fibre levels. GPx4 is critical for the integrity of membranes (Labazi et al., 2015). It is possible that GPx4-mediated membrane repair contributes to the improvement in the *ex vivo* EDL contractile function in *Sod1*KO mice.

To investigate the mechanisms by which overexpression of GPx4 improves muscle contractility in *Sod1*KO mice, we measured force generation in isolated single fibres. We recently reported impaired Ca^{2+} sensitivity of muscle contractile filaments is an important mechanism for muscle weakness in *Sod1*KO mice (Xu et al., 2022). Ca^{2+} sensing and binding on contractile filaments are the important and most direct processes of muscle force generation, and any change in Ca^{2+} sensitivity will result in a significant change in the final force output (Mollica et al., 2012). Results in the current study show that muscles from *Sod1*KO mice are less sensitive to Ca^{2+} signals, and hence will generate less force compared to wild-type muscles in response to the same Ca^{2+} concentration. However, under normal physiological condition, mammalian muscle cells have adaptive mechanisms to avoid high intracellular Ca^{2+} transients following each action potential. This is a protective mechanism to avoid activating Ca^{2+} signal-related degradation pathways, such as calpains or metalloproteinases (Lamb, 2002; Murphy et al., 2006). The relationship between lipid hydroperoxides and muscle calcium homeostasis is not well defined. However, it is possible that reducing lipid peroxidation via the overexpression of GPx4 is responsible for restoring the Ca^{2+} sensitivity and muscle force generation in *Sod1*KO muscles.

Our laboratory and other groups have reported that troponin I regulates Ca^{2+} sensitivity in fast-twitch fibres. Troponin I (TnI) is regulated by Cys134 residue through the modification of *S*-glutathionylation (Mollica et al., 2012; Xu et al., 2018). *S*-Glutathionylation is an adaptive process that commonly occurs after exercise to increase sensitivity to Ca^{2+} ions and produce more force without having to elevate the cytosolic Ca^{2+} concentration to support the short-term demand of a higher force output (Mollica et al., 2012). We uncovered a blunted reaction to *S*-glutathionylation in *Sod1*KO fibres compared to wild-type fibres (Xu et al., 2022), which suggests deleterious oxidative modifications may occur to TnI in *Sod1*KO fibres. Overexpression of GPx4 restored Ca^{2+} sensitivity and force generation following DTDP–GSH treatment which induced *S*-glutathionylation in *Sod1*KO fibres to levels equivalent to wild-type fibres. These data suggest lipid hydroperoxides are a critical

contributor to the deleterious modifications on TnI and to the reduced Ca^{2+} sensitivity in *Sod1*KO fibres.

We also found that depolarization-induced force generation was decreased in *Sod1*KO mice, while depolarization-induced force generation was normal in *Sod1*KO/GPx4 Tg mice. These data suggest that the membrane excitability is impaired in *Sod1*KO mice, and membrane excitability is protected in *Sod1*KO mice with the presence of increased GPx4. In skeletal muscle, the membrane excitability is a key player in triggering force production, and membrane-bound NKA is a key regulator of membrane excitability (Xu et al., 2018). Lipid peroxidation is a major cause of neural inactivation and degeneration, through multiple molecular mechanisms involving cytosolic Ca^{2+} dysregulation and NKA impairment (Chafer-Pericas, 2021). There are two main subunits that comprise the NKA enzyme, NKAα and NKAβ, with NKAα being the catalytic subunit. There are two different isoforms of NKAα with NKAα1 being the ubiquitous isoform appearing in all cell types while NKAα2 is expressed specifically in skeletal muscle. NKA has been reported to be susceptible to oxidative stress, and also it might play a signalling role in regulating redox balance (Bartlett et al., 2018). Consistent with our prior findings, we observed a significant decrease in the amount of NKAα2 in muscles from *Sod1*KO mice (Xu et al., 2022), which may contribute to the poor membrane excitability seen in our fibre experiments. 4-HNE, a by-product of lipid peroxidation, is also able to rapidly bind onto NKA and significantly inhibit its enzymatic activity by damaging the sulfhydryl groups on NKA and forming an NKA–HNE adduct (Morel et al., 1998). Therefore, in addition to restoring NKA content, reducing lipid peroxidation via GPx4 overexpression may improve NKA catalytic activity and membrane excitability in *Sod1*KO muscle by decreasing 4-HNE adducts.

The SERCA pump is crucial for maintaining muscle calcium homeostasis (Xu & Van Remmen, 2021), and oxidative stress reduces SERCA activity (Xu & Van Remmen, 2021). Our prior studies have shown that the SERCA pump plays a vital role in maintaining muscle mass and contractile function in sarcopenic mice (Qaisar et al., 2018). Therefore, we wanted to determine if over-expression of GPx4 improves SERCA function in *Sod1*KO mice. We found that overexpression of GPx4 in *Sod1*KO mice restored the SERCA function to control levels. The improved SERCA function in *Sod1*KO mice with GPx4 overexpression may also contribute to maintaining calcium homeostasis. Although we do not fully understand the direct relationship between lipid hydroperoxides and SERCA function, impaired lipid metabolism, i.e. excessive accumulation of lipid peroxides, will lead to abnormal SR/ER Ca^{2+} homeostasis, which is also known as ‘ER/SR stress’ (Gao et al., 2019).

In conclusion, we have shown that elevated expression of GPx4 improves contractile function in *Sod1*KO mice. We have also shown that GPx4 overexpression improves mitochondrial respiration in *Sod1*KO mice. Further, we have shown that GPx4 maintains membrane excitability and calcium homeostasis in *Sod1*KO mice. Future studies should continue to explore the GPx4-related mechanisms of muscle protection in various muscle pathologies.

Supplementary Material

Refer to Web version on PubMed Central for supplementary material.

Acknowledgements

The authors would like to thank the members of the Van Remmen Laboratory for their contributions to the experiments presented here. The authors would also like to extend our gratitude to the numerous other faculties, staff and other researchers at the Oklahoma Medical Research Foundation, the Oklahoma City VA and OUHSC for helpful discussions.

Funding

J.L.B.'s support for this was provided by VA Career Development Award 1 IK2 BX005620-01A1. H.vR.'s support for this work has been provided by National Institute on Aging R01AG077812 and P01AG051442 and VA merit I01BX004453. H.vR. is also the recipient of a VA Senior Research Career Scientist award (1 IK6 BX005234-01). Contents of this publication are solely the responsibility of the authors and do not necessarily represent the official views of the NIH. J.L.B.'s postdoctoral training was supported by NIA T32 AG052363.

Biography

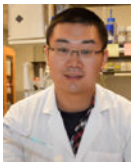

Hongyang Xu obtained his PhD degree in the Department of Biochemistry and Genetics at La Trobe University, Australia, with his research focused on muscle physiological and biochemical alterations induced by sedentary behaviour. He is a post-doctoral fellow in the Aging and Metabolism Program at Oklahoma Medical Research foundation. His broad research interests are ageing-induced high oxidative stress and associated muscle atrophy and weakness, with a particular focus on understanding the subcellular mechanisms related to calcium regulation and its interactions with redox balance in muscle cells. His work is also directed at understanding lipid hydroperoxide-related sarcopenic pathway.

Data availability statement

All raw data will be made available upon request to the corresponding authors.

References

Abrigo J, Simon F, Cabrera D, Vilos C,& Cabello-Verrugio C (2019). Mitochondrial dysfunction in skeletal muscle pathologies. Current Protein & Peptide Science, 20(6), 536–546. [PubMed: 30947668]

Ahn B, Ranjit R, Kneis P, Xu H, Piekarz KM, Freeman WM, Kinter M, Richardson A, Ran Q, Brooks SV, & Van Remmen H (2022). Scavenging mitochondrial hydrogen peroxide by peroxiredoxin 3 overexpression attenuates contractile dysfunction and muscle atrophy in a murine model of accelerated sarcopenia. Aging Cell, 21(3), e13569. [PubMed: 35199907]

Andrade FH, Reid MB, Allen DG, & Westerblad H (1998). Effect of hydrogen peroxide and dithiothreitol on contractile function of single skeletal muscle fibres from the mouse. The Journal of Physiology, 509(2), 565–575. [PubMed: 9575304]

Bartlett D, Miller R, Thiesfeldt S, Lakhani H, Shapiro J, & Sodhi K (2018). The role of Na/K-ATPase signaling in oxidative stress related to aging: Implications in obesity and cardiovascular disease. International Journal of Molecular Sciences, 19(7), 2139. [PubMed: 30041449]

Bhattacharya A, Muller FL, Liu Y, Sabia M, Liang H, Song W, Jang YC, Ran Q, & Van Remmen H (2009). Denervation induces cytosolic phospholipase A2-mediated fatty acid hydroperoxide generation by muscle mitochondria. Journal of Biological Chemistry, 284(1), 46–55. [PubMed: 19001413]

Brigelius-Flohé R (1999). Tissue-specific functions of individual glutathione peroxidases. Free Radical Biology and Medicine, 27(9–10), 951–965. [PubMed: 10569628]

Brown JL, Lawrence MM, Ahn B, Kneis P, Piekarz KM, Qaisar R, Ranjit R, Bian J, Pharaoh G, Brown C, Peelor FF, Kinter MT, Miller BF, Richardson A, & Van Remmen H (2020). Cancer cachexia in a mouse model of oxidative stress. Journal of Cachexia, Sarcopenia and Muscle, 11(6), 1688–1704, [PubMed: 32918528]

Brown JL, Peelor FF, Georgescu C, Wren JD, Kinter M, Tyrrell VJ, O'donnell VB, Miller BF, & Van Remmen H (2022). Lipid hydroperoxides and oxylipins are mediators of denervation induced muscle atrophy. Redox Biology, 57, 102518. [PubMed: 36283174]

Chafer-Pericas C (2021). Lipid peroxidation in neurodegeneration. Antioxidants, 10, 102518.

Czyżowska A, Brown J, Xu H, Sataranatarajan K, Kinter M, Tyrell VJ, O'donnell VB,& Van Remmen H (2023). Elevated phospholipid hydroperoxide glutathione peroxidase (GPX4) expression modulates oxylipin formation and inhibits age-related skeletal muscle atrophy and weakness. Redox Biology, 64, 102761. [PubMed: 37279604]

Deepa SS, Bhaskaran S, Espinoza S, Brooks SV, Mcardle A, Jackson MJ, Van Remmen H, & Richardson A (2017). A new mouse model of frailty: The Cu/Zn superoxide dismutase knockout mouse. Geroscience, 39(2), 187–198. [PubMed: 28409332]

Deepa SS, Van Remmen H, Brooks SV, Faulkner JA, Larkin L, Mcardle A, Jackson MJ, Vasilaki A, & Richardson A (2019). Accelerated sarcopenia in Cu/Zn superoxide dismutase knockout mice. Free Radical Biology and Medicine, 132, 19–23. [PubMed: 30670156]

Ferri E, Marzetti E, Calvani R, Picca A, Cesari M, & Arosio B (2020). Role of age-related mitochondrial dysfunction in sarcopenia. International Journal of Molecular Sciences, 21(15), 5236. [PubMed: 32718064]

Gao X, Guo S, Zhang S, Liu A, Shi L, & Zhang Y (2019). Correction to: Matrine attenuates endoplasmic reticulum stress and mitochondrion dysfunction in nonalcoholic fatty liver disease by regulating SERCA pathway. Journal of Translational Medicine, 17(1), 277. [PubMed: 31434567]

Goodpaster BH, Park SW, Harris TB, Kritchevsky SB, Nevitt M, Schwartz AV, Simonsick EM, Tylavsky FA, Visser M, & Newman AB (2006). The loss of skeletal muscle strength, mass, and quality in older adults: The health, aging and body composition study. Journals of Gerontology. Series A, Biological Sciences and Medical Sciences, 61(10), 1059–1064. [PubMed: 17077199]

Grundy D (2015). Principles and standards for reporting animal experiments in The Journal of Physiology and Experimental Physiology. The Journal of Physiology, 593(12), 2547–2549. [PubMed: 26095019]

Imai H, Koumura T, Nakajima R, Nomura K, & Nakagawa Y (2003). Protection from inactivation of the adenine nucleotide translocator during hypoglycaemia-induced apoptosis by mitochondrial phospholipid hydroperoxide glutathione peroxidase. Biochemical Journal, 371(3), 799–809. [PubMed: 12534348]

Jang YC, Lustgarten MS, Liu Y, Muller FL, Bhattacharya A, Liang H, Salmon AB, Brooks SV, Larkin L, Hayworth CR, Richardson A, & Van Remmen H (2010). Increased superoxide in vivo accelerates age-associated muscle atrophy through mitochondrial dysfunction and neuromuscular junction degeneration. FASEB Journal, 24(5), 1376–1390. [PubMed: 20040516]

Kanning KC, Kaplan A, & Henderson CE (2010). Motor neuron diversity in development and disease. Annual Review of Neuroscience, 33(1), 409–440.

Labazi M, McNeil AK, Kurtz T, Lee TC, Pegg RB, Angeli JPF, Conrad M, & McNeil PL (2015). The antioxidant requirement for plasma membrane repair in skeletal muscle. Free Radical Biology & Medicine, 84, 246–253. [PubMed: 25843658]

Lamb GD (2002). Excitation-contraction coupling and fatigue mechanisms in skeletal muscle: Studies with mechanically skinned fibres. Journal of Muscle Research and Cell Motility, 23(1), 81–91. [PubMed: 12363289]

Lamb GD, & Posterino GS (2003). Effects of oxidation and reduction on contractile function in skeletal muscle fibres of the rat. The Journal of Physiology, 546(1), 149–163. [PubMed: 12509485]

Lamboley CR, Wyckelsma VL, Dutka TL, Mckenna MJ, Murphy RM, & Lamb GD (2015). Contractile properties and sarcoplasmic reticulum calcium content in type I and type II skeletal muscle fibres in active aged humans. The Journal of Physiology, 593(11), 2499–2514. [PubMed: 25809942]

Larkin LM, Davis CS, Sims-Robinson C, Kostrominova TY, Remmen HV, Richardson A, Feldman EL, & Brooks SV (2011). Skeletal muscle weakness due to deficiency of CuZn-superoxide dismutase is associated with loss of functional innervation. American Journal of Physiology. Regulatory, Integrative and Comparative Physiology, 301(5), R1400–R1407. [PubMed: 21900648]

Liang H, Remmen HV, Frohlich V, Lechleiter J, Richardson A, & Ran Q (2007). Gpx4 protects mitochondrial ATP generation against oxidative damage. Biochemical and Biophysical Research Communications, 356(4), 893–898. [PubMed: 17395155]

Liang H, Yoo S-E, Na R, Walter CA, Richardson A, & Ran Q (2009). Short form glutathione peroxidase 4 is the essential isoform required for survival and somatic mitochondrial functions. Journal of Biological Chemistry, 284(45), 30836–30844. [PubMed: 19744930]

Loehr JA, Stinnett GR, Hernández-Rivera M, Roten WT, Wilson LJ, Pautler RG, & Rodney GG (2016). Eliminating Nox2 reactive oxygen species production protects dystrophic skeletal muscle from pathological calcium influx assessed in vivo by manganese-enhanced magnetic resonance imaging. The Journal of Physiology, 594(21), 6395–6405, [PubMed: 27555555]

Mollica JP, Dutka TL, Merry TL, Lamboley CR, Mcconell GK, Mckenna MJ, Murphy RM, & Lamb GD (2012). S-glutathionylation of troponin I (fast) increases contractile apparatus Ca^{2+} sensitivity in fast-twitch muscle fibres of rats and humans. The Journal of Physiology, 590(6), 1443–1463. [PubMed: 22250211]

Morel P, Tallineau C, Pontcharraud R, Piriou A, & Huguet F (1998). Effects of 4-hydroxynonenal, a lipid peroxidation product, on dopamine transport and Na+/K+ ATPase in rat striatal synaptosomes. Neurochemistry International, 33(6), 531–540. [PubMed: 10098723]

Muller FL, Song W, Jang YC, Liu Y, Sabia M, Richardson A, & Van Remmen H (2007). Denervation-induced skeletal muscle atrophy is associated with increased mitochondrial ROS production. American Journal of Physiology. Regulatory, Integrative and Comparative Physiology, 293(3), R1159–R1168. [PubMed: 17584954]

Muller FL, Song W, Liu Y, Chaudhuri A, Pieke-Dahl S, Strong R, Huang T-T, Epstein CJ, Roberts LJ, 2nd, Csete M, Faulkner JA, & Van Remmen H (2006). Absence of CuZn superoxide dismutase leads to elevated oxidative stress and acceleration of age-dependent skeletal muscle atrophy. Free Radical Biology and Medicine, 40(11), 1993–2004. [PubMed: 16716900]

Murphy RM, Verburg E, & Lamb GD (2006). Ca^{2+} activation of diffusible and bound pools of mu-calpain in rat skeletal muscle. The Journal of Physiology, 576(2), 595–612. [PubMed: 16857710]

Pharaoh G, Brown JL, Sataranatarajan K, Kneis P, Bian J, Ranjit R, Hadad N, Georgescu C, Rabinovitch P, Ran Q, Wren JD, Freeman W, Kinter M, Richardson A, & Van Remmen H (2020). Targeting cPLA(2) derived lipid hydroperoxides as a potential intervention for sarcopenia. Scientific Reports, 10(1), 13968. [PubMed: 32811851]

Plant DR, Gregorevic P, Williams DA, & Lynch GS (2001). Redox modulation of maximum force production of fast-and slow-twitch skeletal muscles of rats and mice. Journal of Applied Physiology, 90(3), 832–838. [PubMed: 11181590]

Powers SK, Criswell D, Lawler J, Ji LL, Martin D, Herb RA, & Dudley G (1994). Influence of exercise and fiber type on antioxidant enzyme activity in rat skeletal muscle. American Journal of Physiology, 266(2 Pt 2), R375–R380. [PubMed: 8141392]

Qaisar R, Bhaskaran S, Premkumar P, Ranjit R, Natarajan KS, Ahn B, Riddle K, Claflin DR, Richardson A, Brooks SV, & Van Remmen H (2018). Oxidative stress-induced dysregulation of excitation-contraction coupling contributes to muscle weakness. Journal of Cachexia, Sarcopenia and Muscle, 9(5), 1003–1017. [PubMed: 30073804]

Qaisar R, Bhaskaran S, Ranjit R, Sataranatarajan K, Premkumar P, Huseman K, & Van Remmen H (2019). Restoration of SERCA ATPase prevents oxidative stress-related muscle atrophy and weakness. Redox Biology, 20, 68–74. [PubMed: 30296699]

Ran Q, Liang H, Gu M, Qi W, Walter CA, Roberts LJ, 2nd, Herman B, Richardson A, & Van Remmen H. (2004). Transgenic mice overexpressing glutathione peroxidase 4 are protected against oxidative stress-induced apoptosis. Journal of Biological Chemistry, 279(53), 55137–55146. [PubMed: 15496407]

Schwarzer E, Arese P, & Skorokhod OA (2015). Role of the lipoperoxidation product 4-hydroxynonenal in the pathogenesis of severe malaria anemia and malaria immunodepression. Oxidative Medicine and Cellular Longevity, 2015, 638416. [PubMed: 25969702]

Stifani N (2014). Motor neurons and the generation of spinal motor neuron diversity. Frontiers in Cellular Neuroscience, 8, 293. [PubMed: 25346659]

Tadokoro T, Ikeda M, Ide T, Deguchi H, Ikeda S, Okabe K, Ishikita A, Matsushima S, Koumura T, Yamada K-I, Imai H, & Tsutsui H (2020). Mitochondria-dependent ferroptosis plays a pivotal role in doxorubicin cardiotoxicity. JCI Insight, 5(9), e132747. [PubMed: 32376803]

Xu H, Ahn B, & Van Remmen H (2022). Impact of aging and oxidative stress on specific components of excitation contraction coupling in regulating force generation. Science Advances, 8(43), eadd7377. [PubMed: 36288318]

Xu H, Ranjit R, Richardson A, & Van Remmen H (2021). Muscle mitochondrial catalase expression prevents neuromuscular junction disruption, atrophy, and weakness in a mouse model of accelerated sarcopenia. Journal of Cachexia, Sarcopenia and Muscle, 12(6), 1582–1596. [PubMed: 34559475]

Xu H, Ren X, Lamb GD, & Murphy RM (2018). Physiological and biochemical characteristics of skeletal muscles in sedentary and active rats. Journal of Muscle Research and Cell Motility, 39(1–2), 1–16. [PubMed: 29948664]

Xu H, & Van Remmen H (2021). The SarcoEndoplasmic Reticulum Calcium ATPase (SERCA) pump: A potential target for intervention in aging and skeletal muscle pathologies. Skeletal Muscle, 11(1), 25. [PubMed: 34772465]

Yagi K, Shidoji Y, Komura S, Kojima H, & Ohishi N (1998). Dissipation of mitochondrial membrane potential by exogenous phospholipid monohydroperoxide and protection against this effect by transfection of cells with phospholipid hydroperoxide glutathione peroxidase gene. Biochemical and Biophysical Research Communications, 245(2), 528–533. [PubMed: 9571189]

Key points

- Knockout of CuZn superoxide dismutase (*Sod1*KO) induces elevated oxidative stress with accelerated muscle atrophy and weakness.
- Glutathione peroxidase 4 (GPx4) plays a fundamental role in the reduction of lipid hydroperoxides in membranes, and overexpression of GPx4 improves mitochondrial respiration and reduces hydroperoxide generation in *Sod1*KO mice.
- Muscle contractile function deficits in *Sod1*KO mice are alleviated by the overexpression of GPx4. GPx4 overexpression in *Sod1*KO mice rescues the impaired muscle membrane excitability of fast-twitch muscle fibres and improves their calcium sensitivity.
- Sarco/endoplasmic reticulum Ca^{2+}-ATPase activity in *Sod1*KO muscles is decreased, and it is restored by the overexpression of GPx4.
- Our results confirm that GPx4 plays an important role in preserving excitation–contraction coupling function and Ca^{2+} homeostasis, and maintaining muscle and mitochondrial function in oxidative stress-induced sarcopenia.

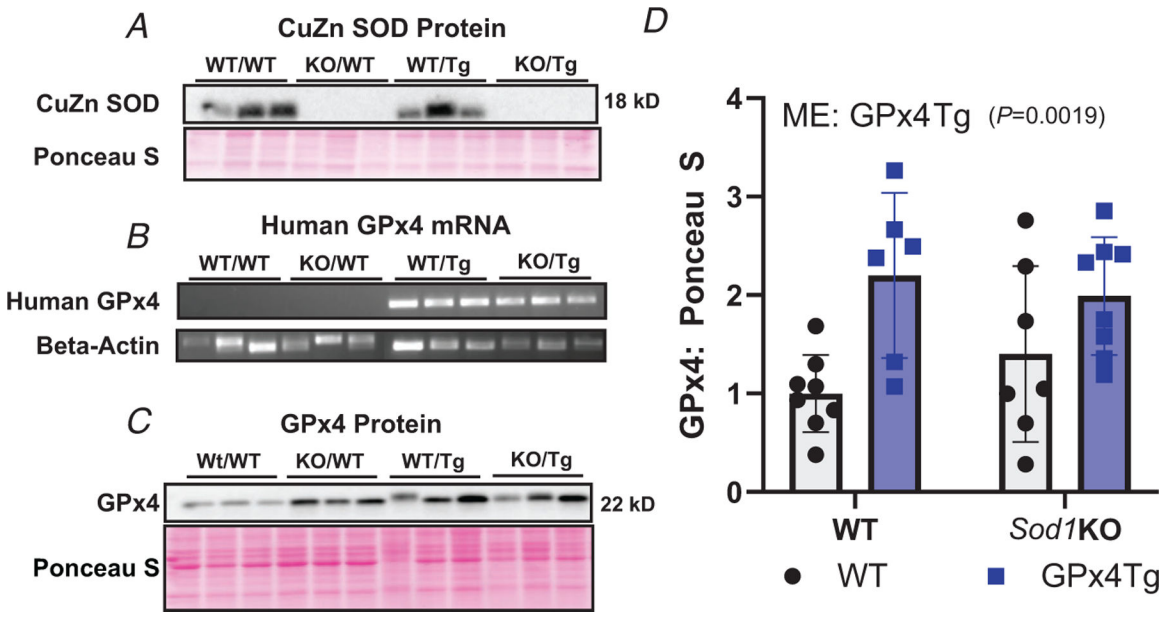

Figure 1. Confirmation of genotype

A, confirmation of deletion of *Sod1*. *B*, mRNA expression of human *GPx4*. *C*, representative image showing GPx4 protein content. *D*, quantification of GPx4 protein content. Main effect (ME): GPx4 Tg $P = 0.0019$, two-way ANOVA. Data are presented as means ± SD, $n = 5–11$ per group. GPx4, glutathione peroxidase 4; Sod1, CuZn superoxide dismutase.

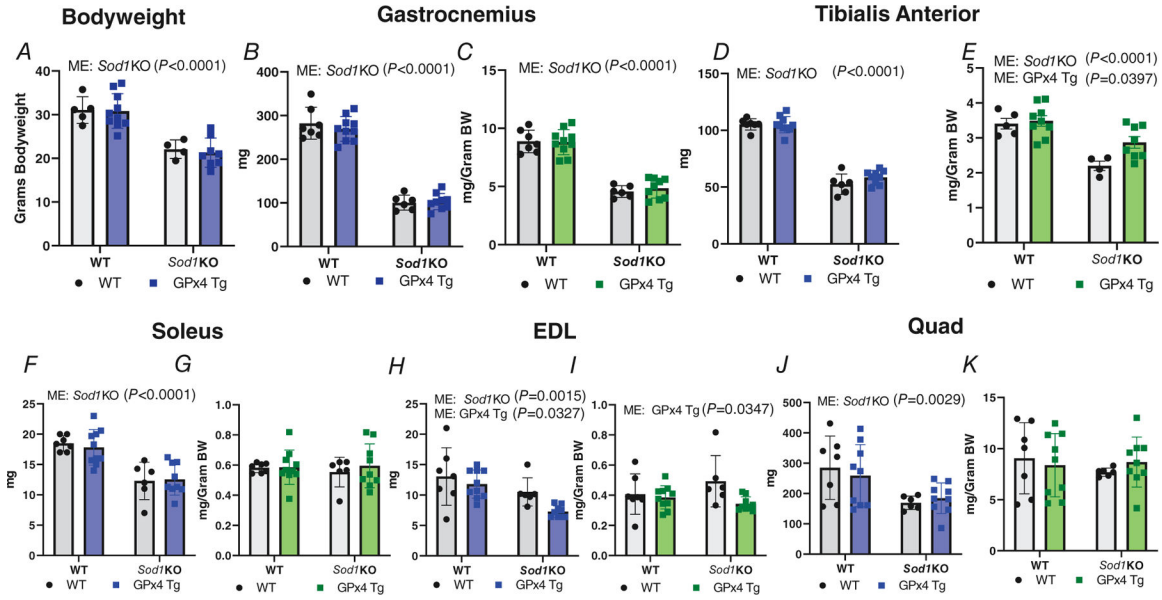

Figure 2. Overexpression of GPx4 does not protect against muscle atrophy in *Sod1*KO mice

A, mouse bodyweights (ME: *Sod1*KO $P < 0.0001$). *B*, absolute gastrocnemius wet weights (ME: *Sod1*KO $P < 0.0001$). *C*, gastrocnemius wet weights normalized to bodyweights (ME: *Sod1*KO $P < 0.0001$). *D*, raw TA wet weights (ME: *Sod1*KO $P < 0.0001$). *E*, TA wet weights normalized to bodyweights (ME: *Sod1*KO $P < 0.0001$; ME GPx4Tg $P = 0.0397$). *F*, absolute soleus wet weights (ME: *Sod1*KO $P < 0.0001$). *G*, soleus normalized to bodyweights. *H*, absolute EDL muscle wet weights (ME: *Sod1*KO $P = 0.0015$; ME: *GPx4Tg* $P = 0.0327$). *I*, EDL normalized to bodyweights (ME: GPx4 Tg $P = 0.0347$). *J*, raw quadriceps muscle wet weights (ME: *Sod1*KO $P = 0.0029$). *K*, quadriceps normalized to bodyweights. Data are presented as means ± SD, $n = 5–11$ per group. Two-way ANOVA was used for global analysis. EDL, extensor digitorum longus; GPx4, glutathione peroxidase 4; Sod1, CuZn superoxide dismutase; TA, tibialis anterior.

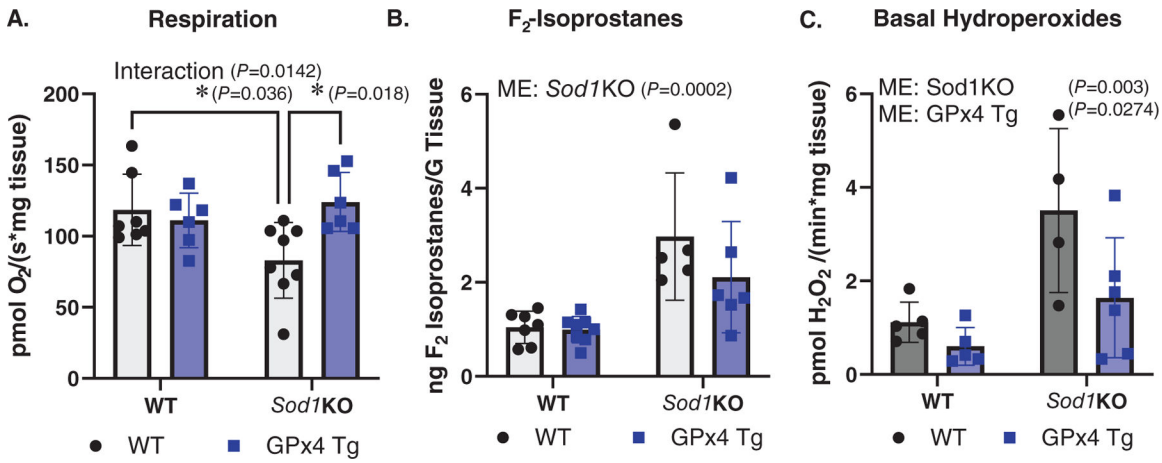

Figure 3. Overexpression of GPx4 in *Sod1*KO mice improves mitochondrial respiration and reduces oxidative damage and reactive oxygen species generation

A, maximally stimulated respiration in permeabilized fibre bundles (interaction $P = 0.0142$). *B*, F_2-isoprostanes measured in quadriceps muscle (ME: *Sod1*KO $P = 0.0002$). *C*, basal hydroperoxide generation measured in permeabilized fibre bundles (ME: *Sod1*KO $P = 0.003$; ME: GPx4 Tg $P = 0.0274$). *Significant difference between labelled groups (two-way ANOVA). Data are presented as means ± SD, $n = 4–8$ per group. GPx4, glutathione peroxidase 4; Sod1, CuZn superoxide dismutase.

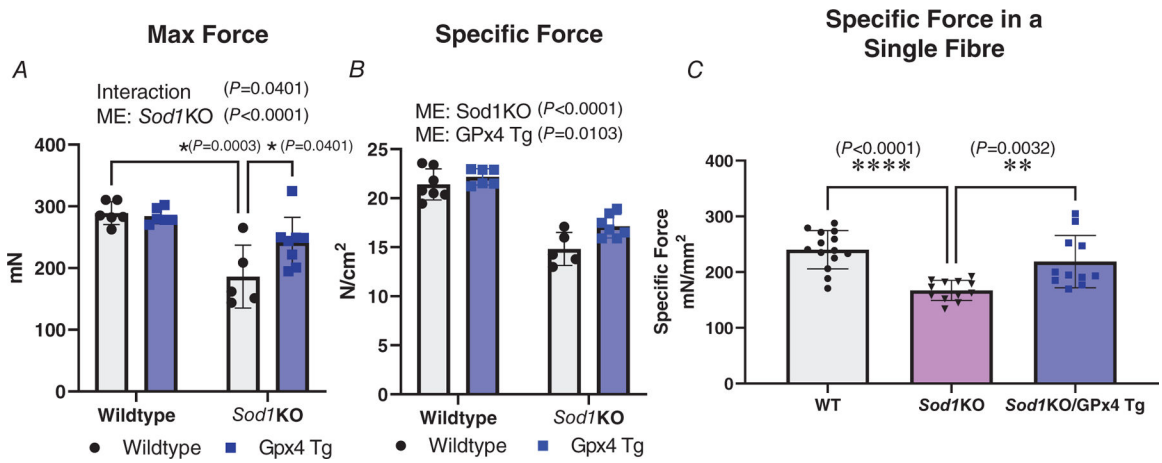

Figure 4. Overexpression of GPx4 improves contractile function in EDL muscle in *Sod1*KO mice

Muscle force production was measured at whole muscle level from EDL muscle with *in vitro* electrical stimulation, or at single skinned fibre level from fast-twitch fibres with Ca^{2+} activation at pCa 4.6. Specific force (N/cm^2 or mN/mm^2) was defined as maximum contraction force (N or mN) normalized to fibre cross-sectional area (cm^2 or mm^2). *A*, maximum muscle force production measured in whole muscle in different groups (interaction $P = 0.0401$; ME: *Sod*1KO $P < 0.0001$). *B*, specific maximum force production measured in whole muscle in different groups (ME: *Sod1*KO $P < 0.0001$; ME: GPx4 Tg $P = 0.0103$). *C*, specific maximum force production measured in single fibres in different groups. *Significant difference between labelled groups ($P = 0.0032$) (*A* and *B*, two-way ANOVA; *C*, one-way ANOVA). $n = 5–8$ animals per group was used for *A* and *B*. Data are presented as means ± SD; $n = 11–14$ fibres analysed, $n = 3–4$ animals from which the fibres were obtained. GPx4, glutathione peroxidase 4; Sod1, CuZn superoxide dismutase.

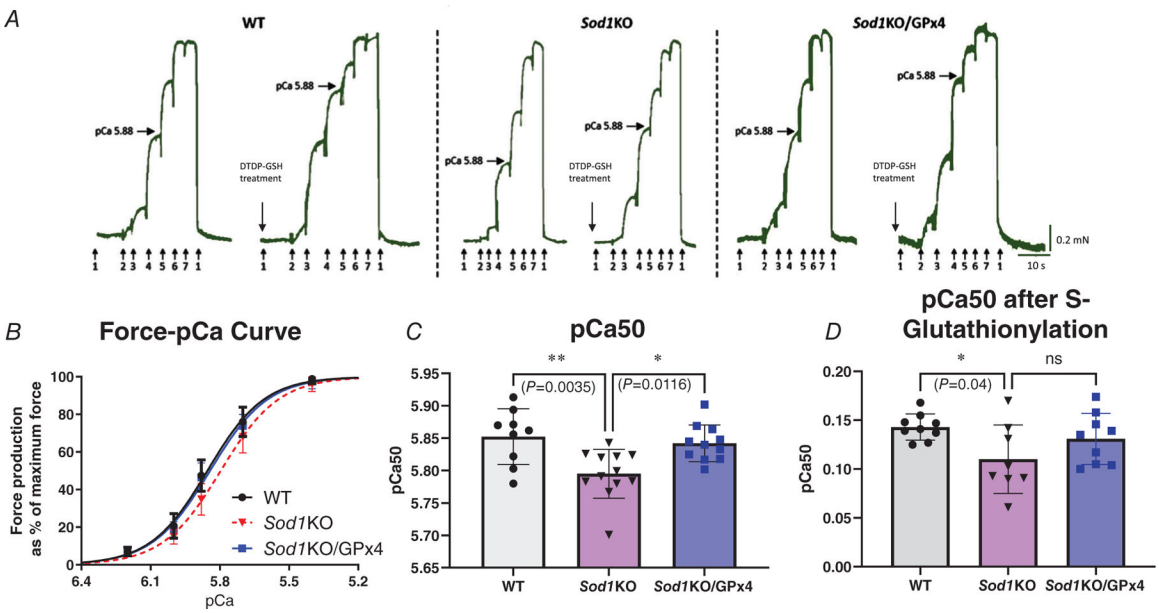

Figure 5. Overexpression of GPx4 improves calcium sensitivity of contractile filaments in fast-twitch fibres in *Sod1*KO mice, as well as the activating reaction to *S*-glutathionylation

Individual skinned muscle fibres from fast-twitch muscles of different groups were activated in a series solution with progressively higher free [Ca^{2+}] from pCa >10 to 4.7 (denoted by arrows: 1 (pCa >10, no force), 2 (pCa 6.2), 3 (pCa 6.0), 4 (pCa 5.88), 5 (pCa 5.7), 6 (pCa 5.4), 7 (pCa 4.7, maximum Ca^{2+}-activating solution)). Horizontal arrows mark force level achieved at pCa 5.88. DTDP–GSH treatments were applied at pCa >10 with 100 μM DTDP for 5 min followed by 5 mM GSH for 2 min. *A*, representative force traces of single skinned fast-twitch fibres from WT, *Sod1*KO and *Sod1*KO/GPx4 mice, before and after DTDP–GSH treatment (*S*-glutathionylation). *B*, force–pCa curves of different groups. *C*, pCa_{50} values (i.e. pCa giving half-maximum force) for individual fast-twitch muscle fibres in different groups with and without *S*-glutathionylation ($P = 0.0032$, $P = 0.0116$). *D*, changes in Ca^{2+} sensitivity (ΔpCa_{50}) with *S*-glutathionylation treatments in fast-twitch fibres from different groups ($P = 0.04$, ($P = 0.24$)). *Significant difference between labelled groups (one-way ANOVA). Data are presented as means ± SD; $n = 8–9$ fibres analysed, $n = 3–4$ animals from which the fibres were obtained. GPx4, glutathione peroxidase 4; Sod1, CuZn superoxide dismutase.

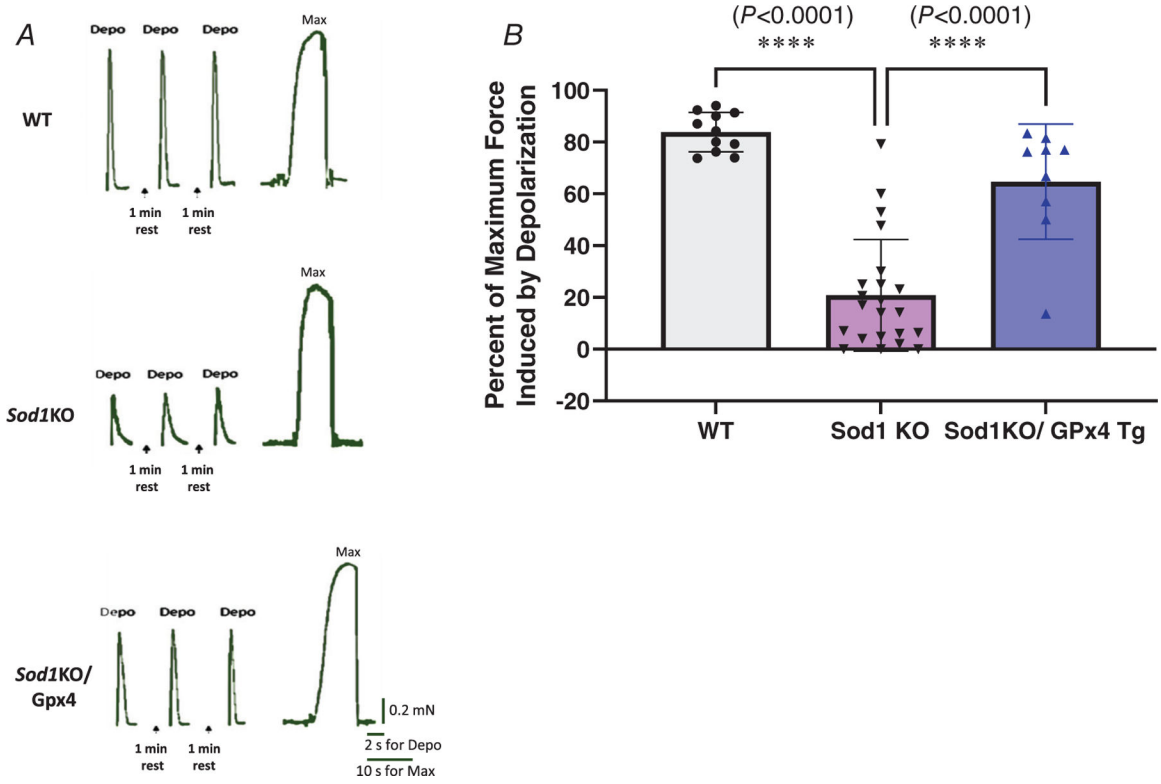

Figure 6. Membrane excitability is significantly impaired in fast-twitch fibres from *Sod1*KO mice and greatly improved by the overexpression of GPx4

A, representative force traces of single skinned fast-twitch fibres from WT, *Sod1*KO and *Sod1*KO/GPx4 mice during depolarization. *B*, depolarization-induced force generation. *Significant difference between labelled groups ($P < 0.0001$, one-way ANOVA). Values are expressed as means ± SD; $n = 9–22$ fibres analysed, $n = 6–7$ animals from which the fibres were obtained. GPx4, glutathione peroxidase 4; Sod1, CuZn superoxide dismutase.

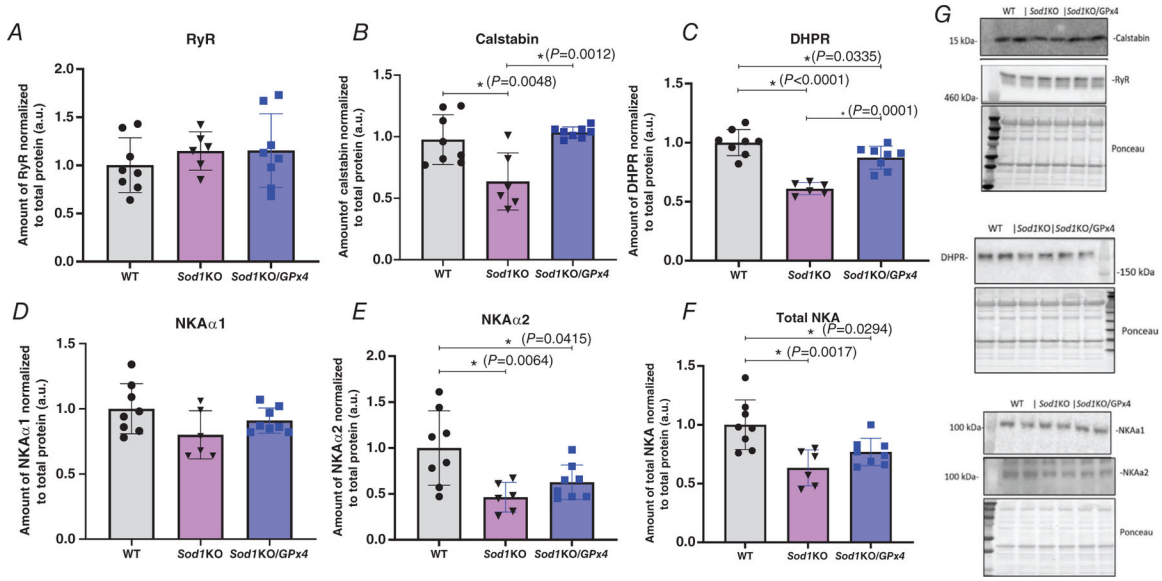

Figure 7. GPx4 overexpression alters the expression of excitation-related proteins in *Sod1*KO mice

A, RYR protein content. *B*, calstabin protein content ($P = 0.0048$, $P = 0.0012$). *C*, DHPR protein content ($P < 0.0001$, $P = 0.0335$, $P = 0.0001$). *D*, NKAα1 protein content. *E*, NKAα2 protein content ($P = 0.0064$, $P = 0.0415$). *F*, total NKA protein content ($P = 0.0017$, $P = 0.0294$). *G*, representative western blot images. *Significant difference between labelled groups (one-way ANOVA). Values are expressed as means ± SD, $n = 6–7$ animals. GPx4, glutathione peroxidase 4; Sod1, CuZn superoxide dismutase.

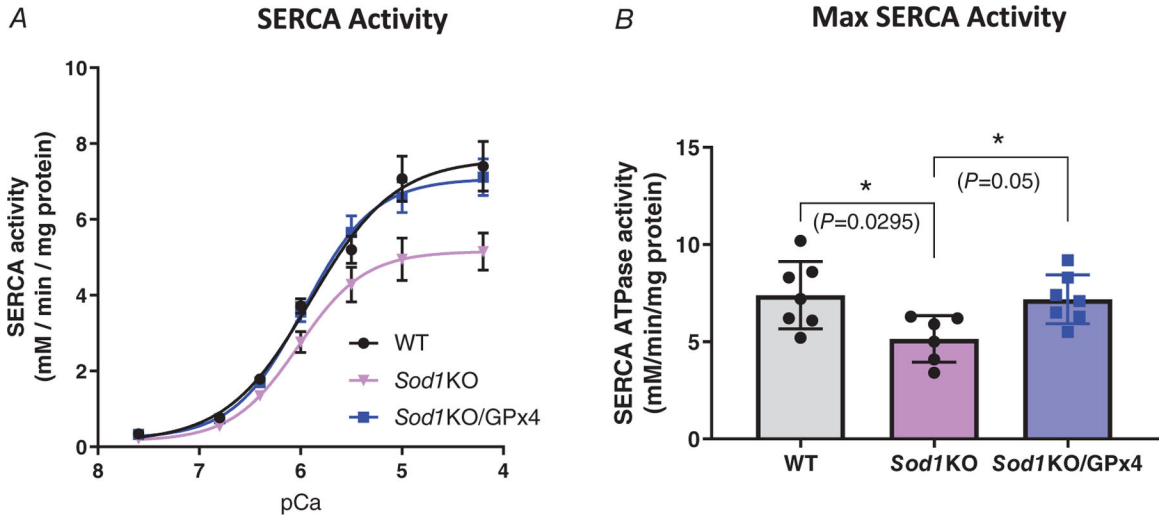

Figure 8. Overexpression of GPx4 in *Sod1*KO mice improves SERCA activity

SERCA activity was measured in homogenates of quadriceps muscle from different groups. *A*, SERCA activity and pCa curves. *B*, maximal SERCA activity ($P = 0.0295$, $P = 0.05$). *Significant difference between labelled groups (one-way ANOVA). Values are expressed as means ± SD, $n = 6–7$ animals. GPx4, glutathione peroxidase 4; Sod1, CuZn superoxide dismutase.